

Modeling Cd-free buffer layer and defects analysis in CZTS solar cell

SAURABH KUMAR PANDEY

Department of Electrical Engineering, Indian Institute of Technology, Patna-801103, Bihar, India

A compact numerical evaluation and optimization for CZTS ($\text{Cu}_2\text{ZnSnS}_4$) solar cell has been done using device simulation software. Various factors affecting the solar cell's performance has been rigorously investigated; more specifically physical parameters of buffer and absorber layer. By optimizing the device parameters we have achieved a simulated conversion efficiency of 15.6% with open circuit voltage (V_{oc}) = 0.8V, short circuit current density (J_{sc}) = 26.4 mA/cm² and a fill factor (FF) = 79.7%. The role of defect density has been also studied to analyze the performance of cell module and comparative analysis with alternative buffer material (ZnIn_2Se_4) has also been discussed. The solar cell with an absorber layer's thickness of 2 μm , an acceptor concentration of 1×10^{16} cm⁻³ and buffer layer's thickness of 70nm was optimum. Compared to one of the best-reported values of conversion efficiency from CdS based CZTS films available in the literature, we have obtained improved performance parameters of the cell module. The optimization of device parameters outperforms most experimental devices by a large margin, indicating that there may possibly be huge potential for the improvement for conversion efficiency of CZTS solar cell.

(Received October 8, 2013; accepted August 3, 2016)

Keywords: CZTS solar cell, Conversion efficiency, Energy band, MgZnO, ZnIn_2Se_4

1. Introduction

Polycrystalline thin-film solar cells have reached a high level of interest on photovoltaic market because of their high efficiency and low production costs. Among various thin film solar cells, CZTS which consist of naturally abundant materials, are very promising candidate for high efficiency, low cost, non-toxic and rare metal-free solar cells for solar photovoltaic conversion purposes [1,2]. CZTS is the I₂-II-IV-VI₄ quaternary compound semiconductor with excellent photovoltaic properties such as, tunable band gap energy of 1.4-1.56 eV and high absorption coefficient (10^4 cm⁻¹), which are highly desired in photovoltaic material. $\text{Cu}_2\text{ZnSnS}_4$ (CZTS) is a prominent low cost absorber layer to be used as a substitute of CIGS absorber layer [3]. The light to electricity conversion efficiency of $\text{Cu}_2\text{ZnSnS}_4$ -based solar cells has increased from 0.66% in 1996 to almost 10% in 2010 [4,5]. However, due to the quaternary phase the structural, crystallographic, and electrical properties can be influenced by stoichiometric composition, which will result in formation of native defects [6]. Device performance of thin film CZTS solar cell is very sensitive to variations in buffer layer. The presence of toxic cadmium poses environmental concerns that prompted research efforts aimed at replacing the CdS buffer with Cd-free layers. In order to control the conduction band offset, we proposed the use of $\text{Mg}_x\text{Zn}_{1-x}\text{O}$ film as the window layer of the CZTS solar cell. In this aspect, MgZnO has proven to be suitable replacement for CdS, due to its wide band gap and convenient band alignment

with the CZTS absorber [7]. Changes in this MgZnO layer results in a notable impact on the device energy-conversion efficiency. The $\text{Mg}_x\text{Zn}_{1-x}\text{O}$ band gap has a great impact in terms of band alignment and therefore of conversion efficiency [8-10]. $\text{Mg}_x\text{Zn}_{1-x}\text{O}$ has been used as a barrier layer for the modulation of band gap to enhance light transmission. Thus n-MgZnO can be employed as a buffer layer in CZTS solar cells. It also helps to increase the current generation of solar cell [11].

Several research groups have attempted the various physical and chemical techniques to fabricate the CZTS solar cell including RF magnetron sputtering [12], pulse laser deposition [13], thermal evaporation [14], co-sputtering [15], sol-gel method [16] etc. Despite the progress of device performance (conversion efficiency) and experimental techniques; there are limited investigations to understand the important design parameters needed to optimize for high efficiency solar cells. The device performance study is mainly based on the material parameters, optical parameters, and electrical parameters of each layers used in the structure.

In order to optimize the device parameters; a comprehensive study of CZTS solar cell has been done to identify the important parameters for quick assessment and high performance of cell module. A detailed theoretical model of Cd-free CZTS module has been analyzed and device parameters have been varied to study the electrical and optical parameters. Finally defects analysis and buffer material (ZnIn_2Se_4) have been compared with MgZnO layer to analyze the photovoltaic device parameters.

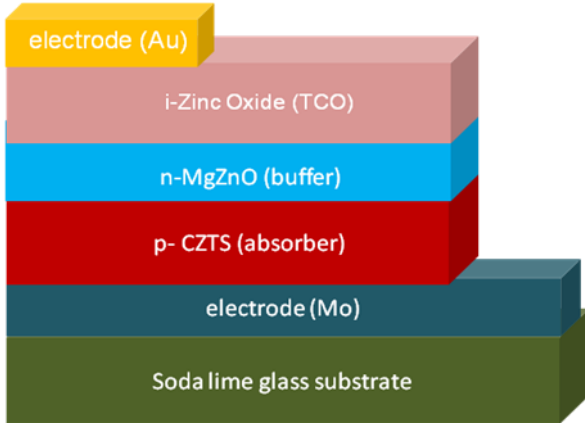


Fig.1. Schematic diagram of simulated thin film CZTS solar cell

2. Device structure

The vertical cross section of thin film CZTS solar cell is illustrated in Fig. 1. The two layers that have been emphasized in this modeling were buffer layer and absorber layer. On top of the substrate, Mo has been taken as a back contact layer as it has high optical absorption coefficient (10^5 cm^{-1}) and reduces the reflection losses. p-type CZTS layer has been deposited over the molybdenum, which is the absorber (active) layer of this device. An MgZnO buffer layer has been used on the top of absorber layer to reduce the absorption losses and to increase transmittance. The MgZnO buffer layer will show significant increase in efficiency with illumination time. For cells with ZnO buffer layers, light-soaking mainly causes an increase in V_{oc} while for Mg-rich buffers the major effect is an improvement in fill factor. A transparent ZnO contact layer has also been used to obtain good electrical conductivity. Here, we have chosen transfer matrix method to simulate AM1.5 conditions sampled between 0.3 microns and 1.2 microns at 50 samples and the default operation temperature is set to 300K. The various base parameters used in this simulation study is summarized in Table I [12, 17].

The discrete spectrum $I_{dis}(\lambda_i)$ calculated from the standard AM1.5 spectrum, $I_{AM1.5}(\lambda)$, by:

$$I_{dis}(\lambda_f) = \int_{\lambda_2}^{\lambda_1} I_{AM1.5}(\lambda) d\lambda \quad (1)$$

Where $I_{AM1.5}(\lambda)$ is given in the units of photons per area*time*wavelength.

All measurements used air mass 1.5 (AM1.5) illuminations, which delivers a power density P_{inc} 100 mW/cm^2 . The band offsets at the interfaces can be given in terms of difference of electron affinities. For conduction band offsets:

$$\Delta E_{C1} = \chi_{MgZnO} - \chi_{ZnO} \quad \Delta E_{C2} = \chi_{CZTS} - \chi_{MgZnO} \quad (2)$$

The fill factor and efficiency of solar cell can be calculated by

$$FF = \frac{P_{max}}{J_{sc} V_{oc}} = \frac{J_m V_m}{J_{sc} V_{oc}} \quad (3)$$

$$\eta = \frac{J_m V_m}{P_{inc}} \quad (4)$$

where J_{sc} , V_{oc} and P_{inc} are short circuit current density, open circuit voltage and incoming power density respectively.

Table 1: Material parameters used in the simulation study for CZTS solar cell. All parameters were taken at room temperature.

Parameters	i-ZnO	n-Mg _x Zn _{1-x} O	p-CZTS
Layer Thickness	40 nm	70 nm	2 μm
Recombination lifetime			
Electrons, sec	1×10^{-7}	6.5×10^{-9}	1×10^{-9}
Holes, sec			1×10^{-9}
Electron Affinity	4.6	4.05	4.5
DOS* in conduction band (cm^{-3})	2.2×10^{18}	1.8×10^{19}	2.2×10^{18}
DOS in valence band (cm^{-3})	1.8×10^{19}	2.4×10^{18}	1.8×10^{19}
Dielectric Permittivity (eV)	9	10.5	10
Band gap (eV)	3.37	4.1	1.5
Electron mobility, $\text{cm}^2 \text{V}^{-1} \text{s}^{-1}$	100	400	100
Hole mobility, $\text{cm}^2 \text{V}^{-1} \text{s}^{-1}$	25	50	25

DOS* - Density of states

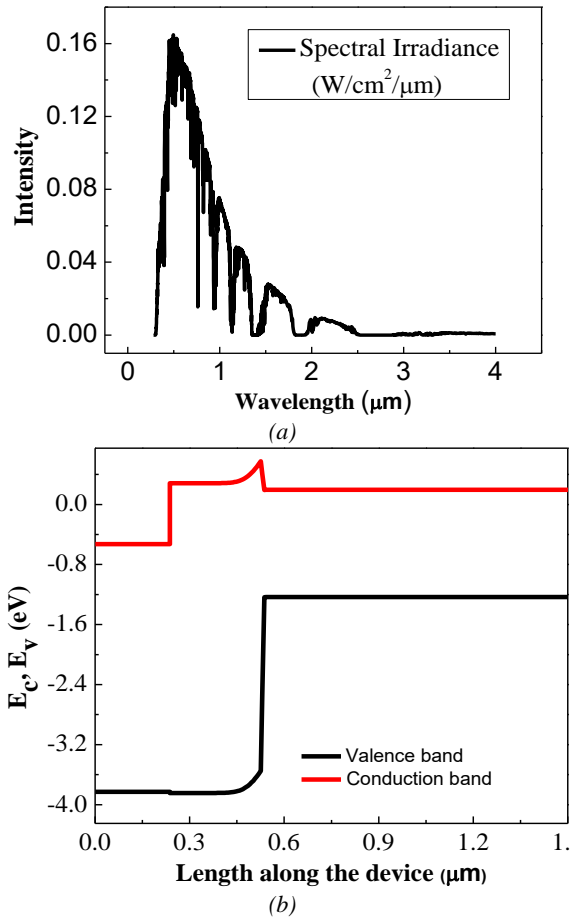


Fig. 2. (a) AM1.5 spectrum and (b) Energy band diagram of CZTS structure module.

The standard terrestrial spectrum used in photovoltaic research is approximately AM 1.5 [18] which has been shown in fig. 2(a). The p-n junction in CZTS cell is formed between the p-type CZTS absorber and n type MgZnO buffer layer. The energy band diagram for CZTS cell module is shown in fig. 2(b).

The thickness of absorber layer has been varied from 500 nm to 2 μm to study the dependency of output parameters of CZTS solar module. We investigated the effects of layer thickness on the cell performance parameters such as J_{sc} , V_{oc} , efficiency and fill factor, as shown in fig. 3. J_{sc} and V_{oc} both increases with the CZTS layer thickness. As the thickness of absorber layer is increased, more electron-hole pairs will be generated and more photons with longer wavelength will be absorbed by the active region (absorber). Hence, J_{sc} and V_{oc} will increase and finally efficiency will be improved. Since it would not be cost effective to produce CZTS solar cells with very large absorber thickness, thus tradeoff should be maintained between cell efficiency and cost for mass production. The simulated conversion efficiency of this CZTS model is 15.6%, which can be subjected to experimental verification with a precise control of the process parameters for improving the performance of CZTS thin film solar cell.

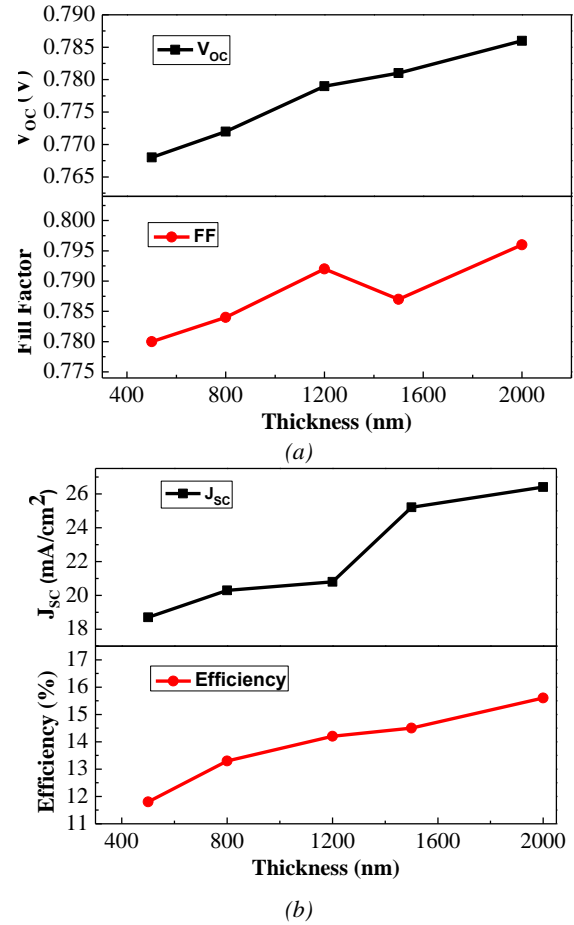


Fig. 3. (a) Open circuit voltage and fill factor (b) Short circuit current density and power conversion efficiency variation as a function of CZTS layer thickness

3. CZTS cell modeling

Device modeling helps us to understand certain device properties and processes that take place in solar cell operation. The modeling has been performed using the commercial TCAD simulation software [19]. For each one of these layers, material parameters has been optimized in order to best match the available device technology under the condition of air mass 1.5 global (AM1.5G) illumination and default operation temperature is set to 300K. The basic semiconductor equations considered in such a simulation are Poisson's and continuity equations for electrons and holes [20]. We have studied the performance dependency of geometrical parameters such as doping concentration and thickness for the thin film CZTS solar cell to achieve the optimum value of power conversion efficiency. All other physical parameters are held constant; when any one of the parameter is varied. Compared to one of the best-reported values of conversion efficiency from CdS based CZTS films available in the literature, we have obtained improved performance parameters of the CZTS solar cell [21].

3.1 Buffer layer

a) Doping concentration

In this CZTS solar cell, MgZnO acts as a buffer layer. The first design parameter to consider for the $Mg_xZn_{1-x}O$ buffer layer is Mg doping concentration since its band gap is linearly increases with concentration. Increasing the effective carrier concentration in the MgZnO layer broadens the conduction band thus increases the band gap and leads to overall higher barrier [8]. It can be observed from fig.4 that as we increase the Mg concentration from 5×10^{16} to $5 \times 10^{18} \text{ cm}^{-3}$, the open circuit voltage remains nearly unchanged while power conversion efficiency decreases due to recombination of photo generated carriers.

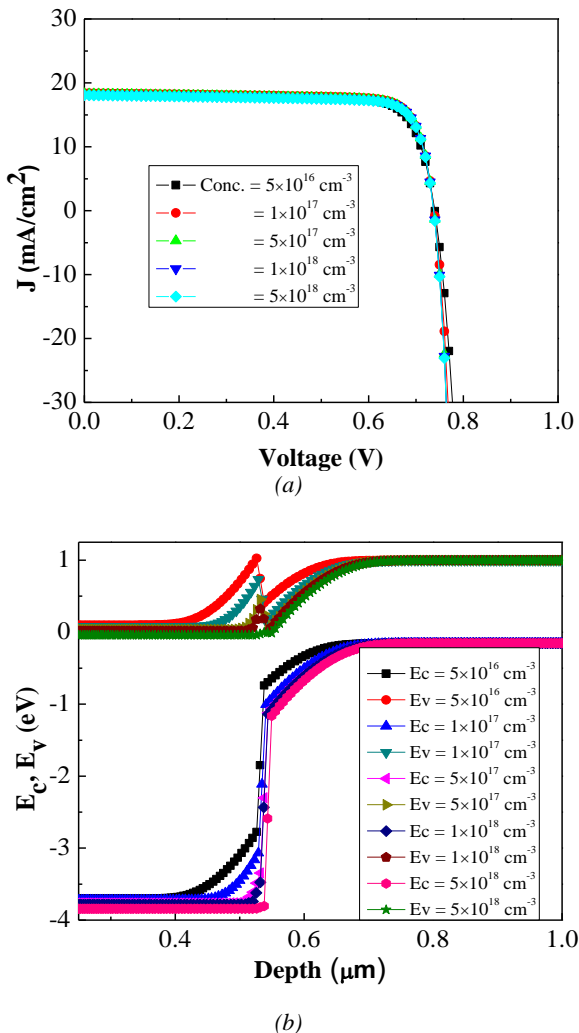


Fig. 4. Simulated (a) J-V characteristic (b) Energy band MgZnO/CZTS interface as a function of donor concentration of buffer layer of CZTS solar cell.

b) Layer thickness

The second design parameter for the simulation is buffer layer thickness in this study. Changes in MgZnO layer thickness influence the J-V and PCE curves, since

there exist considerable absorption of photons ($E_{\text{photon}} > E_G^{MgZnO} = 4.1 \text{ eV}$) in this layer. Due to its wide band gap, more high energy photons will be absorbed by MgZnO layer. Thus more electron-hole pairs are generated. Finally J_{sc} will increase, which improves the quantum efficiency of solar cell as shown in the fig.5.

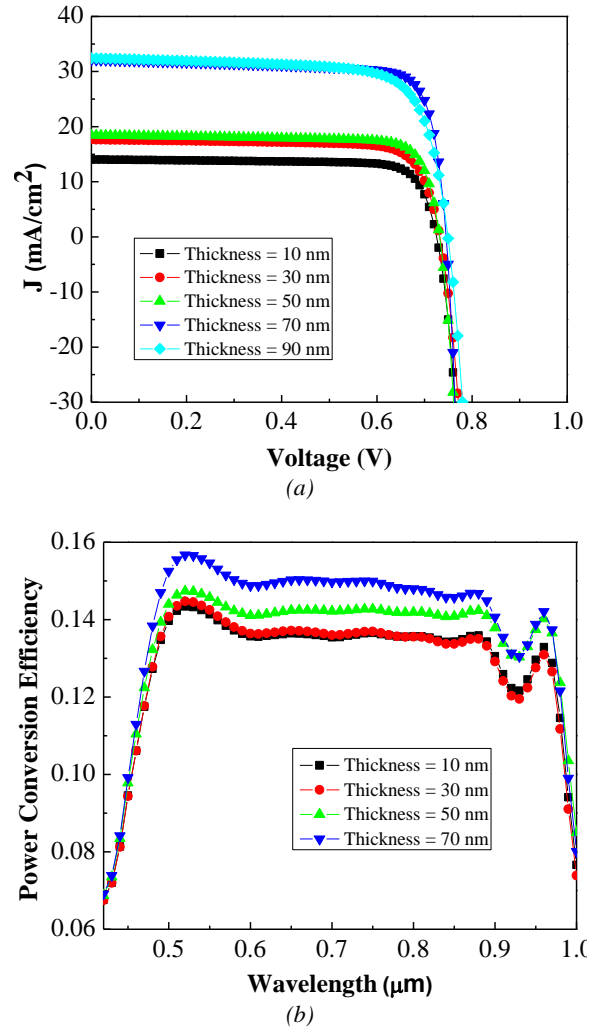


Fig. 5. Simulated (a) J-V characteristic and (b) Power conversion efficiency as a function of thickness of buffer layer of CZTS solar cell.

3.2 Absorber layer

a) Doping concentration

It can be observed from Fig.6 that as we increase the doping concentration from 1×10^{15} to $1 \times 10^{17} \text{ cm}^{-3}$, Cu deficiency increases the majority carrier concentration by increasing the number of Cu vacancies. These vacancies act as electron acceptors. This reduces the short circuit current density (J_{sc}) to 17.5 mA/cm^2 which leads to degradation of power conversion efficiency to 8%.

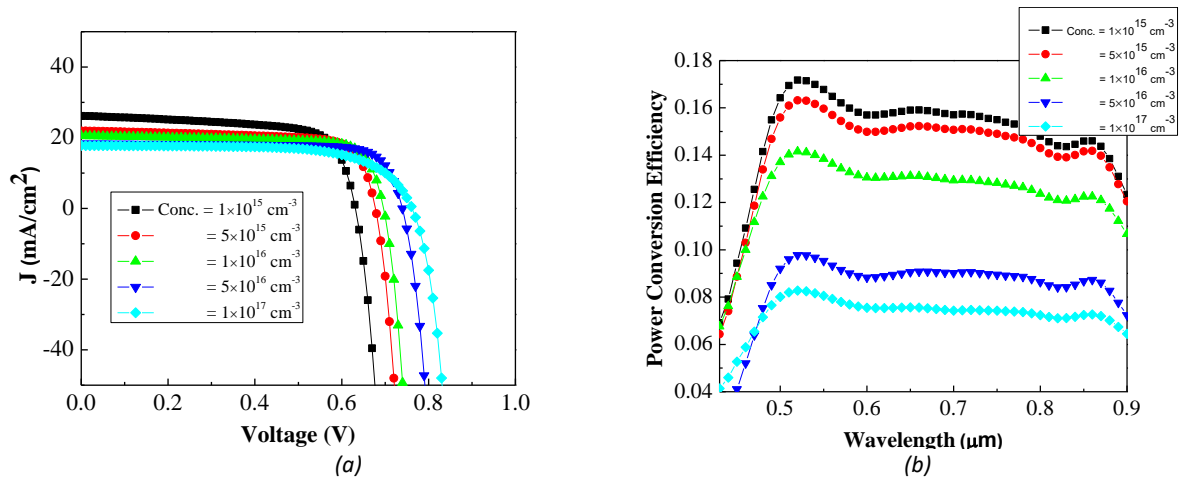


Fig. 6. Simulated (a) J - V characteristic (b) Power conversion efficiency as a function of acceptor concentration of absorber layer of CZTS solar cell.

b) Layer thickness

As seen from Fig.7 when the thickness of absorber layer increases from 500 nm to 2000 nm, the recombination probability of the photon generated carriers with back contact decreases. Recombination depends on the junction depth. As the thickness of the layer increases, the junction depth decreases while both open circuit voltage (V_{oc}) and short circuit current density (J_{sc}) increases relative to the thickness of the layer. Therefore, the photo generated carriers are collected efficiently at

higher thickness of the absorber layer [17]. Efficiency spectra shown in fig. 7 suggest that at higher thickness of the CZTS absorber layer the maximum photon generated carriers are being collected and gives maximum 15.6 % photon conversion efficiency. Our simulation shows that thickness up to 2 μ m is sufficient for absorption of AM 1.5G radiation gap due to high absorption coefficient and direct band gap.

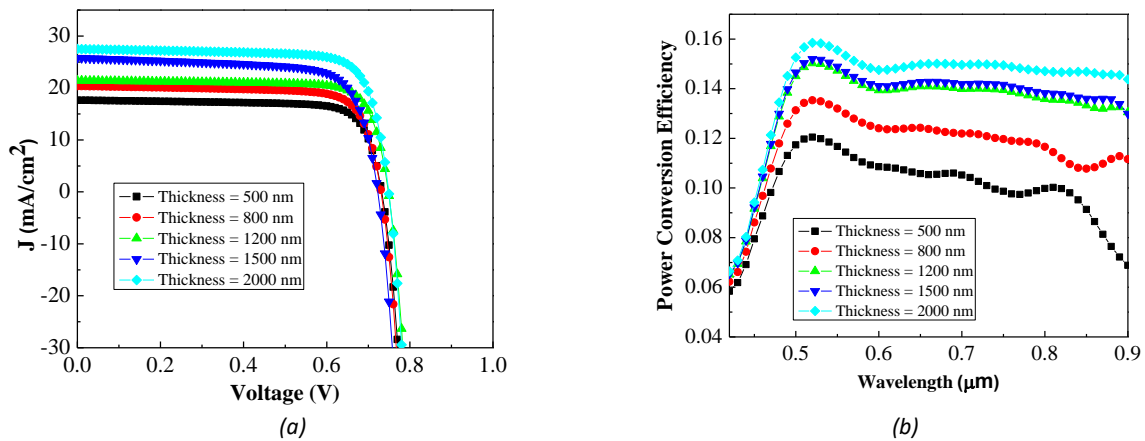


Fig. 7. Simulated (a) J - V characteristic and (b) power conversion efficiency as a function of thickness of absorber layer of CZTS solar cell.

4. Defect density analysis

The output parameters depend strongly on the number of defects and their capture cross-sections. As far as dominance of acceptor type defect of the CZTS thin film is concerned, it is highest due to the Cu-deficient site. The device modeling has been also performed with and without inclusion of mid-gap defect density states.

The defects are assumed donor-like in the ZnO and CZTS, and acceptor-like in the MgZnO. As seen from Fig.8 when the defects are introduced, the power conversion efficiency degrades from 15.6% to 14.2%. Similarly, the short circuit current density reduces from 41.4 mA/cm² to 20.6 mA/cm² on considering the defects into the cell module.

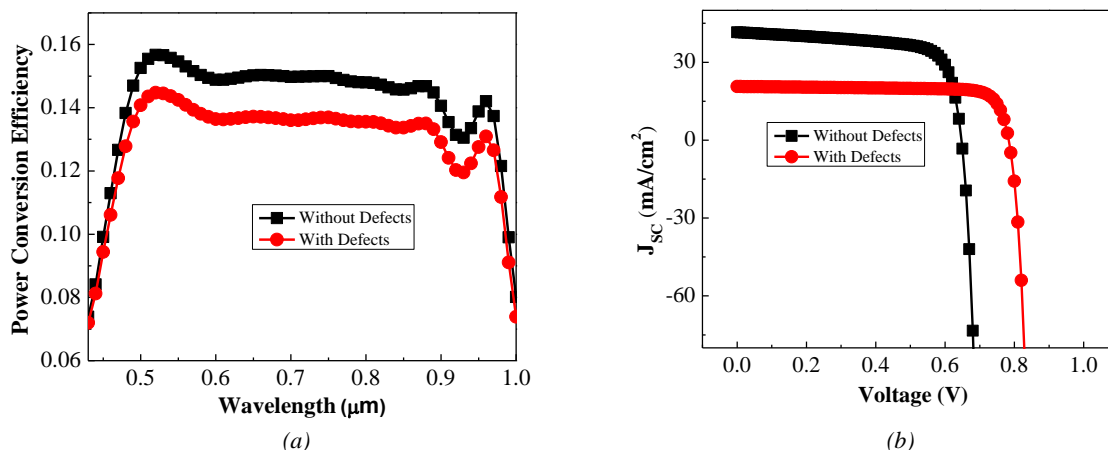


Fig. 8. Simulated (a) Power conversion efficiency (b) J-V characteristic as a function of with and without defect states of CZTS solar cell.

Fig. 9 shows the conversion efficiency and J-V graph of simulation with ZnIn_2Se_4 buffer, which are being compared with MgZnO buffer layer. The short circuit current density J_{sc} of cell with MgZnO buffer is greater than that of CZTS cell with ZnIn_2Se_4 buffer. This could be attributed to interface defects or lattice mismatch between the ZnIn_2Se_4 and CZTS material of the solar cell, which could leads to degradation of overall performance of cell module.

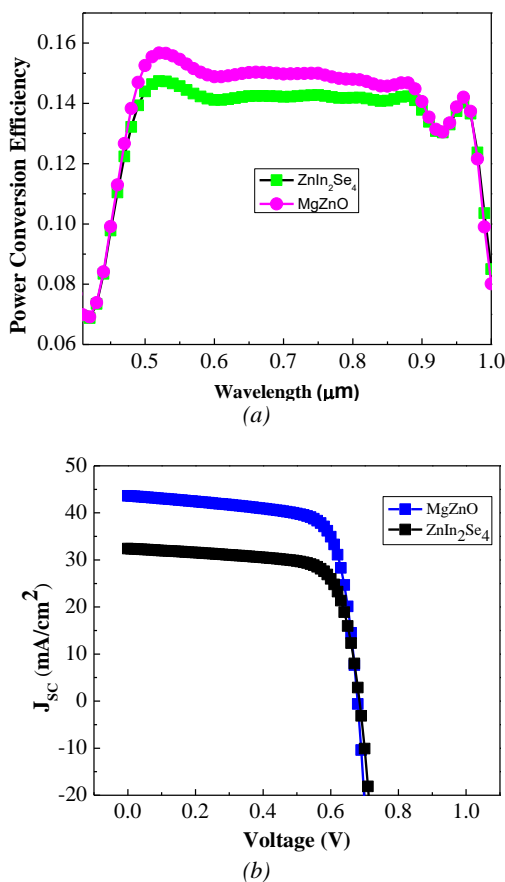


Fig. 9. Simulated (a) Power conversion efficiency (b) J-V characteristic of CZTS solar cell with ZnIn_2Se_4 and MgZnO buffer layer.

5. Conclusion

This paper presents an effort of understanding the operation of CZTS solar cell as a function of different parameters with an adjusted model based on fundamental principle. In this work, we have studied the influence of MgZnO buffer and absorber layer parameters modifications on CZTS solar cell properties. From the simulation results, it has been found that the thick absorber layer and thin buffer layer results in higher conversion efficiency of solar cell. Furthermore, thickness of MgZnO buffer layer and absorber layer has been found 70 nm and 2 μm as the optimum. The present optimized results give helpful indication for experimental verification with precise control of process parameters. We found that ZnIn_2Se_4 can also be used as alternate buffer materials in the production of CZTS solar cells.

Acknowledgement

The ATLAS device simulation software used here for simulation was provided by IIT Indore.

References

- [1] H. Katagiri, K. Jimbo, W. S. Maw, K. Oishi, M. Yamazaki, H. Araki, A. Takeuchi, *Thin Solid Films* **517**, 2455 (2009).
- [2] Jian Li, Hui Du, John Yarbrough, Andrew Norman, Kim Jones, Glenn Teeter, Fred Lewis Terry, Dean Levi, *Optics Express* **20**, A327 (2012).
- [3] Qijie Guo, M. Grayson, Ford, Wei-Chang, Yang, Bryce, C. Walker, Eric A. Stach, W. Hillhouse Hugh, Rakesh Agrawal, *J. Am. Chem. Soc.* **132**, 17384 (2010).
- [4] H. Katagiri, K. Jimbo, W. S. Maw, K. Oishi, M. Yamazaki, H. Araki, A. Takeuchi, *Thin Solid Films* **517**, 2455 (2009).

- [5] J. Scragg, P. Dale, L. Peter, *Thin Solid Films* **517**, 2481 (2009).
- [6] S. Chen, J. H. Yang, X. G. Gong, A. Walsh, S. H. Wei, *Phys. Rev. B.* **81**, 245204 (2010).
- [7] I. Repins, M. A Contreras, B. Egaas, C. Dehart, J. Scharf, C. L. Perkins, R. Noufi, *Progress in Photovoltaics: Research and Applications* **16**, 235 (2008).
- [8] Jae Won Kim, Hong Seong Kang, Jong Hoon Kim Sang Yeol Lee, Jung-Kun Lee, Michael Nastasi, *J. of Appl. Phys.* **033701**, 100 (2006).
- [9] P. Zabierowski, C. Platzer-Bjorkman, *Proc. of the 22nd Euro. Photovoltaic Solar Energy Conference*, p. 2395 (2007).
- [10] T. Minemoto, T. Hashimoto, Y. Satoh, T. Negami, T. Takakura, H. Y. Hamakawa, *J. Appl. Phys.* **89**, 8327 (2001).
- [11] T. Minemoto, Yasuhiro Hashimoto, Wahid Shams-Kolahi, Takuya Satoh, Takayuki Negami, Hideyuki Takakura, Yoshihiro Hamakawa, *Solar Energy Mat. & Solar Cells.* **75**, 121 (2003).
- [12] J. Seol, S. Lee, J. Lee, H. Nam, K. Kim., *Solar Energy Mat. & Solar Cells.* **75**, 155 (2003).
- [13] A. V. Moholkar, S. S. Shinde, A. R. Babar, K. U. Sim, Y. B. Kwon, K. Y. Rajpure, P. S. Patil, C. H. Bhosale, J. H. Kim, *Solar Energy* **85**, 1354 (2011).
- [14] K. Wang, O. Gunawan, T. Todorov, B. Shin, S. J. Chey N. A. Bojarczuk, D. Mitzi, S. Guha, *Appl. Phy. Lett.* **97**, 143508-3 (2010).
- [15] H. Katagiri, K. Jimbo, W. S. Maw, K. Oishi, M. Yamazaki Hideaki Araki, Akiko Takeuchi, *Thin Solid Films.* **517**, 2455 (2009).
- [16] N. Moritake, Y. Fukui, M. Oonuki, K. Tanaka, H. Uchiki, *Phy. Stat. Solidi (c)* **6**, 1233 (2009).
- [17] M. Gloeckler, A. L. Fahrenbruch, J. R. Sites, *Proc. of 3rd World Conference on Photovoltaic Energy Conversion.* p. 491, 2003.
- [18] American society for testing and materials, *Standard for Terrestrial Direct Normal Solar Spectral Irradiance tables for Air Mass 1.5, West Conshocken, PA, USA.*
- [19] *ATLAS User's Manual, Device Simulation Software.* Santa Clara, CA: SILVACO International, 2009.
- [20] M. Burgelman, P. Nollet, S. Degrave, *Thin Solid Films* **527**, 361(2000).
- [21] Malkesh Kumar Patel, Abhijit Ray, *Physica B.* **407**, 4391 (2012).

*Corresponding author: saurabh@iitp.ac.in